

A Measurement of Time-Averaged Aerosol Optical Depth using Air-Showers Observed in Stereo by HiRes

R.U. Abbasi,¹ T. Abu-Zayyad,¹ J.F. Amann,² G. Archbold,¹ R. Atkins,¹ K. Belov,¹ J.W. Belz,³ S. BenZvi,⁵ D.R. Bergman,⁶ J.H. Boyer,⁴ C.T. Cannon,¹ Z. Cao,¹ B.M. Connolly,⁵ Y. Fedorova,¹ C.B. Finley,⁵ W.F. Hanlon,¹ C.M. Hoffman,² M.H. Holzscheiter,² G.A. Hughes,⁶ P. Hüntemeyer,¹ C.C.H. Jui,¹ M.A. Kirn,³ B.C. Knapp,⁴ E.C. Loh,¹ N. Manago,⁷ E.J. Mannel,⁴ K. Martens,¹ J.A.J. Matthews,⁸ J.N. Matthews,¹ A. O'Neill,⁵ K. Reil,¹ M.D. Roberts,⁸ S.R. Schnetzer,⁶ M. Seman,⁴ G. Sinnis,² J.D. Smith,¹ P. Sokolsky,¹ C. Song,⁵ R.W. Springer,¹ B.T. Stokes,¹ S.B. Thomas,¹ G.B. Thomson,⁶ D. Tupa,² S. Westerhoff,⁵ L.R. Wiencke,¹ A. Zech⁶
 (The High Resolution Fly's Eye Collaboration)

Corresponding author email: wiencke@cosmic.utah.edu

February 5, 2008

ABSTRACT

Air fluorescence measurements of cosmic ray energy must be corrected for attenuation of the atmosphere. In this paper we show that the air-showers themselves can yield a measurement of the aerosol attenuation in terms of optical depth, time-averaged over extended periods. Although the technique lacks statistical power to make the critical hourly measurements that only specialized active instruments can achieve, we note the technique does not depend on absolute calibration of the detector hardware, and requires no additional equipment beyond the fluorescence detectors that observe the air showers. This paper describes the technique, and presents results based on analysis of 1258 air-showers observed in stereo by the High Resolution Fly's Eye over a four year span.

Subject headings: HiRes, extensive air-showers, atmosphere, aerosols, aerosol optical depth

¹University of Utah, Department of Physics and High Energy Astrophysics Institute, Salt Lake City, UT 84112, USA.

²Los Alamos National Laboratory, Los Alamos, NM 87545, USA.

³University of Montana, Department of Physics and Astronomy, Missoula, MT 59812, USA.

⁴Columbia University, Nevis Laboratories, Irvington, NY 10533, USA.

⁵Department of Physics, Columbia University, New York, NY 10027, USA.

⁶Rutgers — The State University of New Jersey, Department of Physics and Astronomy, Piscataway, NJ 08854, USA.

⁷University of Tokyo, Institute for Cosmic Ray Research, Kashiwa City, Chiba 277-8582, Japan.

⁸University of New Mexico, Department of Physics and

1. Introduction

Fluorescence detectors use the atmosphere calorimetrically to measure the energy deposited by extensive air-showers. Ultra-violet fluorescence emitted by particle cascades can be observed tens of kilometers away by a photosensitive detector when the primary cosmic particle is above 10^{18} eV. The energy of the primary particle is measured in proportion to the total number of photons yielded by the shower.

Monitoring atmospheric clarity is required to calibrate for atmospheric propagation losses of light between the shower and the detector. Ob-

Astronomy, Albuquerque, NM 87131, USA.

taining this calibration requires routine measurements by specialized equipment, generally lasers, and LIDARS. While essential, this equipment is challenging to construct, maintain, and calibrate, especially in the remote deserts where fluorescence detectors are located. Active systems are limited in their beams can not be so bright as to swamp the fluorescence detectors and cause saturation of the data acquisition systems. Additional methods to measure the aerosol optical depth and cross-check these conventional measurements can be helpful, especially when no additional equipment is needed.

The High Resolution Fly’s Eye observatory (HiRes), located at Dugway, Utah, USA features two fluorescence detector stations separated by 12.6 km. (See Abu-Zayyad (2000) and Boyer (2002).) Each station views nearly the full azimuth. The HiRes-1 station has one ring of telescopes that view 3.5 to 16 degrees of elevation. A second ring of telescopes extends the elevation coverage of the HiRes-2 station to 30 degrees. Each telescope features a 3.75 m^2 mirror that focuses light onto a camera of 256 photomultiplier tubes (PMTs). Each PMT views approximately ($1^\circ \times 1^\circ$).

The atmosphere is modeled using molecular scattering and ozone absorption as a baseline. The remaining attenuation is attributed to aerosols. The HiRes experiment includes steerable lasers used to measure aerosol attenuation. For more details, see Abassi (2005).

This paper describes an independent measurement of aerosol optical depth that uses air-showers viewed in stereo. It has the advantage that it is insensitive to the absolute photometric calibration of the detector hardware and the total fluorescence yield that are two of the largest uncertainties of the fluorescence technique. In the sense that air-showers are a natural part of the primary data sample, the technique incurs no additional cost. Furthermore, the measurement is made over the band of wavelengths that air-showers produce, and for the range of distances over which HiRes measures air-showers. Nor does this analysis require a comprehensive reconstruction of the air-shower light profile, energy, or primary particle composition; it is enough to reconstruct the shower axis, identify segments of the shower viewed in common by two detectors, and apply a set of selection cri-

teria.

We note that the technique has limitations. The relatively low flux of extensive air-showers restricts the statistical power of the technique to the measurement of one parameter, total aerosol optical depth, averaged over years. To reduce sensitivity of the result to details of the aerosol vertical distribution, the technique assumes that most of the aerosol is distributed below the shower segments used in the analysis. The assumption is supported by an analysis of laser shots (Abassi 2005), that found that the aerosol vertical distribution is consistent with an average scale height of about 1 km. For this analysis we use shower segments at least 1 km above the detectors.

2. Stereo light balance method

For stereo observations of atmospheric events to yield consistent results between detectors, an accurate description of the atmospheric attenuation is required. Conversely, a consistency constraint can be used to find the total optical depth.

Here we use a molecular description of the atmosphere as a baseline and apply a consistency constraint to find the remainder optical depth due to atmospheric aerosols.

2.1. General solution

The aerosol atmosphere is modeled with a total aerosol optical depth τ . A ray traveling vertically to infinity is attenuated by one exponent of τ . A inclined ray traveling to an altitude z is attenuated

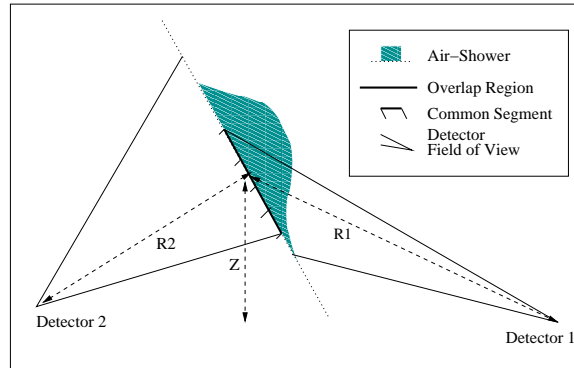


Fig. 1.— Diagram of a cosmic ray air-shower as viewed in stereo.

by

$$T = e^{\left(-\frac{\tau}{\sin \alpha} \left[1 - e^{-\frac{z}{SH}} \right] \right)}, \quad (1)$$

where T is transmission, α is the elevation angle of the ray, and SH is the Scale Height of the aerosol distribution.

A useful parameter η can be factored out of this expression.

$$T = e^{(-\tau\eta)} \quad (2)$$

$$\eta = \frac{1}{\sin \alpha} \left[1 - e^{-\frac{z}{SH}} \right] \quad (3)$$

Equation 3 gives us a particular definition of η applicable to this model for monochromatic light in the aerosol atmosphere. However, the argument that follows requires only that η be a known parameter that satisfies Equation 2.

Suppose that a segment of an extensive air-shower (Figure 1) produces N optical photons and some number, S_D , are recorded by a fluorescence detector during atmospheric conditions that are less than perfectly clear (i.e. through aerosol haze). Had conditions been perfectly clear (i.e. molecular with no aerosol) a greater fraction of the photons produced would have reached the detector. Thus the same measured value of S_D would have corresponded to a smaller number, N_M , of photons produced, where $N_M < N$.

N_M depends on the detected signal and, by definition, does not depend on the aerosol property we wish to measure. It can be calculated using $N_M = S_D * f$, where f is a function of the measured shower-detector geometry, and molecular optical depth. The latter can be calculated from molecular scattering theory and knowledge of the atmospheric density profile derived from radiosonde data. N and N_M are related by $N = N_M/T$, ignoring multiple scattering effects.

When two detectors observe the same shower segment, two simultaneous equations can be written.

$$N(1) = N_M(1)e^{(\tau\eta(1))} \quad (4)$$

$$N(2) = N_M(2)e^{(\tau\eta(2))} \quad (5)$$

We constrain the two detectors to agree on the number of photons emitted, $N(1) = N(2)$, and solve to find the light balance equation

$$\Delta_N = \tau\Delta_\eta, \quad (6)$$

where 'light balance' $\Delta_N \equiv \ln \left(\frac{N_M(1)}{N_M(2)} \right)$ and 'event asymmetry' $\Delta_\eta \equiv \eta(2) - \eta(1)$.

It follows that a plot of Δ_N versus Δ_η for a sample of events will have a slope of τ .

2.2. Polychromatic approximation

Any application of the light balance equation (6) requires a definition of η which fits the attenuation model involved and satisfies Equation 2. Equation 3 provides a definition of η which is suitable if the light source is monochromatic. However for polychromatic light in the atmosphere it is not possible to satisfy Equation 2 with a simple definition of η . This difficulty is rooted in the wavelength dependence of scattering. Aerosol optical depth τ is approximately inversely proportional to wavelength. Molecular scattering follows a much steeper relationship.

For convenience, we will refer to the aerosol optical depth at 355 nm as $\tau \equiv \tau(355)$, with the understanding that depths at other wavelengths can be scaled from this value.

A good approximate solution is found by making a guess τ' close to τ and redefining

$$\eta = -\frac{\ln \left(\frac{N_M}{N'} \right)}{\tau'}, \quad (7)$$

where N' is the number of photons emitted by the event assuming τ' , and N_M is the number of photons emitted assuming a molecular atmosphere (not including τ').

This definition rigorously satisfies Equation 2 only if $\tau' = \tau$, and in general it may be necessary to apply this solution iteratively to converge on a value of τ , unless the approximation is particularly good. The quality of the approximation depends primarily on the spectral bandwidth.

In the study that follows, the sensitivity of τ with respect to τ' is less than 1:100. We will set τ' to 0.040 for the remainder of the discussion, since this uncertainty is much smaller than other errors in the analysis.

2.3. Line sources

Equation 6 applies to point sources of light in a straightforward fashion. An air-shower has a cross section hundreds of meters wide and is observed more than 10 km away, and can be considered a

point source traveling at the speed of light. A simpler approach in practice, is to treat the air-shower as a line source.

A line source can be treated by integrating an infinite number of point sources along the line segment. Equation 6 can be applied this way, provided that Δ_η is relatively constant over the segment.

In this analysis, air-shower tracks are split until Δ_η varies by 0.3 or less over the track segments. Detector pixel size is sometimes a limitation in splitting the tracks. If the variation in Δ_η can't be kept below 1.0, the event is removed from the data.

2.4. Data Selection

Data from the HiRes detectors is matched by trigger time to produce stereo candidates. These candidates are passed through a Rayleigh filter to select track-like events while removing various noise triggers. Candidates may also be cut if a shower-detector plane can not be fit. We start this analysis with 5217 stereo shower candidates collected between December 1999 and December 2003.

From the stereo candidates we select 1258 events for light balance analysis that have well reconstructed geometries and a common region observed by both detectors. Depending on the length of the common region, it may be divided into segments. Tabulations for real and simulated data are provided in Table 1 and the selection criteria is described below.

- 1) Sometimes the two detectors view different segments of track. These events must be cut, since there is no overlapping region.
- 2) Events that saturate the high gain FADC channels at HiRes-2 are dropped.
- 3) A random walk model is used to remove noise events.
- 4) The reconstructed trajectory is required to be downward.
- 5) If a track is very short, there is large uncertainty in the shower-detector plane and therefore a potentially large uncertainty in stereo geometry. Tracks are required to cover at least 4 degrees in each detector.
- 6) If the opening angle is small between the two shower-detector planes, then there is large un-

certainty in the intersection. Events with plane angles less than 8 or larger than 172 degrees are cut.

- 7) Asymmetric Cherenkov scattering is a concern when the track is viewed at an oblique angle. Viewing angles below 30 or above 165 degrees are cut.
- 8) To minimize the effects of any potential asymmetries, the maximum difference in viewing angle is set at 50 degrees.
- 9) To reduce Cherenkov contribution and place observations above most aerosol, the segment altitude must be greater than 1000 m above detectors.
- 10) Equation 6 can be applied to a linear track provided that Δ_η is approximately constant over the track. Track segments are cut if the variance in Δ_η across their length is greater than 1.0.

3. Systematic Error

Systematic errors in this analysis can not result from calibration uncertainties of the detector hardware in the following sense. A wavelength independent calibration scalar, k , applied to Equation (5a).

$$\ln \left(k \times \frac{N(m)_1}{N(m)_2} \right) = \tau (\eta_2 - \eta_1) \quad (8a)$$

$$\ln \left(\frac{N(m)_1}{N(m)_2} \right) = \tau (\eta_2 - \eta_1) - \ln(k) \quad (8b)$$

becomes an additive constant ($\ln(k)$). This error would shift the points in Figure 2 up or down, but would not alter the slope (τ). k could represent an error in overall gain in one or both HiRes detectors, for example. A time dependent shift in calibration could smear the data vertically thus reducing the sensitivity of the slope measurement.

Systematic errors can arise from effects that correlate with the aerosol optical path asymmetry Δ_η . In this regard, we have examined the sensitivity of the slope measurement to a number of sources of uncertainty. Their sum in quadrature is 0.014 (see Table 2).

The aerosol vertical distribution is modeled with a 1.0 km scale height, motivated by HiRes laser measurements Abassi (2005). A variation in the average scale height by ± 0.3 km shifts the value by ± 0.008 . To estimate the effect of the Cherenkov light on the measurement, we generated a sample of simulated showers without the

TABLE 1
SELECTION OF REAL AND SIMULATED STEREO DATA.

Filter	Events	Segments	MC events	MC segments
0. Starting sample (see text).	5217	-	9474	-
1. Require commonly viewed segment(s)	2219	5492	5095	12174
2. High gain channel is not saturated.	1876	4440	4211	9694
3. Rayleigh filter	1810	4290	4199	9674
4. Track trajectory is downward.	1803	4276	4162	9619
5. Track length is 4 degrees in each detector.	1738	4211	3979	9436
6. Stereo plane opening angle is 8 - 172 degrees.	1683	4089	3834	9090
7. The viewing angle is between 30 and 165 degrees.	1572	3413	3458	7222
8. The viewing angle asymmetry is less than 50 degrees.	1472	3200	3230	6625
9. Altitude of segment is above 1000 m.	1362	2656	2929	5462
10. Segment spans less than 1.0 in Δ_η .	1258	2503	2696	5142

Cherenkov component. τ changed by 0.009.

A number of other effects were also investigated. To estimate sensitivity to wavelength dependence effects in detector response, the shower data was reanalyzed with the calibration scaled by $\pm 10\%$ per 100 nm. The difference in τ was found to be ∓ 0.002 . The analysis and simulation used a fluorescence spectrum derived from the measurements of Kakimoto (1996) and the compilation of A. Bunner (1967). Using the more recent spectrum of Nagano (2004) shifts τ by 0.002. Uncertainty in the shower axis geometry arising from the shower-detector plane resolution contributes an error of less than 0.002 to τ . To estimate effects of light transmission via atmospheric multiple scattering, the data was reanalyzed with an estimated contribution to each shower using the formalism of Roberts (2004). The shift in τ was 0.003. Finally, we include an estimated error of 0.005 that arises from the non-linear response of an older model preamp used in some of the HiRes1 mirrors.

4. Results

Figure 2 shows plots of Δ_N versus Δ_η for real data and three Monte Carlo sets. Each point corresponds to a segment of track.

The data is binned in Δ_η . Each bin is fit to a Gaussian to determine a mean and σ in Δ_N . The mean values each bin are weighted by the number of entries and fit to a straight line. Statistical uncertainties are quoted with the slopes.

Monte Carlo data is generated using random geometries and primary particle energies, with lower energies weighted to approximate the measured

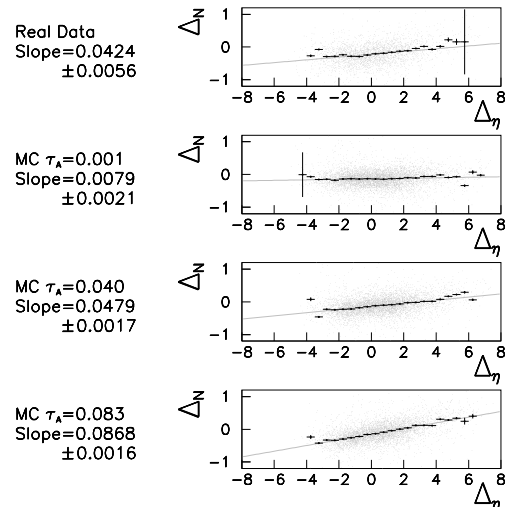


Fig. 2.— Plots of Δ_N (light balance) versus Δ_η (aerosol optical path asymmetry) for real data, and three Monte Carlo sets. According to equation 6, the slope of each plot should be equal to τ . The MC sets are generated using a constant τ of 0.0010, 0.0400, and 0.0833. Linear fits are made to a profile histogram, shown in black.

TABLE 2
SYSTEMATIC ERROR ESTIMATES.

Effect	Approximate error to τ
Cerenkov contribution	0.009
Vertical aerosol distribution	0.008
Preamp non-linearity	0.005
Multiple scattering	0.003
Detector wavelength dependence	0.002
Geometric reconstruction	0.002
Fluorescence spectrum	0.002
Quadrature sum	0.014

HiRes energy spectrum. Three simulated samples are generated using three different values of τ . These are listed with the results in Figure 2. Identical reconstruction and analysis are applied to real and simulated data samples.

The resulting fit for the real data yields an average τ of $(0.042 \pm 0.006(stat) \pm 0.014(sys))$

4.1. Cross check

It is simple to check the accuracy of an atmospheric model by plotting light balance as a function of path difference ($\Delta_r = r(2) - r(1)$). (see diagram in Figure 1.) If the atmospheric model is accurate, the slope should be zero. Figure 3 shows real data reconstructed with three model atmospheres ($\tau = 0.001, 0.040$, and 0.100). A positive slope will indicate a deficit in the an optical depth of the model, while a negative slope indicates an excess.

The plot with $\tau = 0.04$ has a small positive slope, indicating a τ somewhat larger than 0.04, which is consistent with 0.042 shown in Figure 2.

5. Conclusion

Stereo cosmic ray showers are used to measure τ in a manner that is independent of absolute detector calibration. While it cannot replace the hourly and daily measurements obtained by specialized equipment, this method gives a cross check of the amount of aerosols present as averaged over extended periods. This technique may be of use to other experiments that measure air-showers with more than one fluorescence detector station. A trade-off between sensitivity and statistics is expected, depending on the distance between stations. We note, in passing, that this work is the

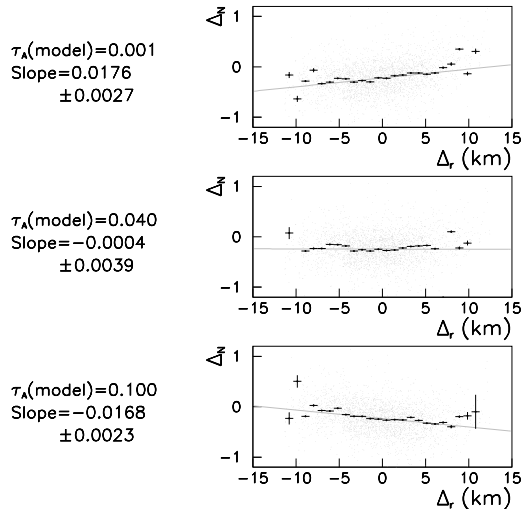


Fig. 3.— Plots of Δ_N (light balance) versus Δ_r (path difference) for real data using three different model atmospheres ($\tau = 0.001, 0.040$, and 0.100). The model with $\tau = 0.040$ results in the smallest slope.

first reported systematic use of air-showers to estimate atmospheric clarity.

REFERENCES

Abu-Zayyad et al. Nucl. Instr. and Meth., A450, (2000) 253.

Abassi et al. (astro-ph/0512423) Accepted for publication in Astroparticle Physics (2005).

Bunner, A. Ph.D. Thesis, Cornell Univsity (1967).

Kakimoto et al., Nucl. Instr. Meth. A372 (1996) 527.

Nagano et al., Astroparticle Physics, V22 (2004) 235.

Longtin, D. R. 1998, Air Force Geophysics Laboratory, AFL-TR-88-0112.

M. Roberts, Pierre Auger GAP Note GAP2004-48, revised version submitted to J. Phys. G.

J. Boyer, et al, Nucl. Instr. and Meth, A482 (2002) 457.

This 2-column preprint was prepared with the AAS L^AT_EX macros v5.2.